# An Absorber-Wall Parallel-Plate Waveguide

C. M. KNOP, SENIOR MEMBER, IEEE, Y. B. CHENG, MEMBER, IEEE, AND E. L. OSTERTAG, MEMBER, IEEE

*Abstract*—**The electromagnetic fields that can propagate through a parallel-plate waveguide having absorber walls are investigated, and it is shown that dominant $TM_{10}^e$ and $TE_{10}^e$ modes can propagate independently with both having: a highly-tapered (cosine-type) transverse distribution, a phase velocity slightly exceeding the speed of light, and very low axial attenuation, especially for a wall-spacing large as compared to a free-space wavelength. In other words, such an absorber-guide acts like a corrugated waveguide having "$\lambda/4$" teeth (balanced-hybrid mode) but it does so over virtually an unlimited bandwidth and with little sensitivity to the absorber's characteristics.**

## I. Introduction

THE SEARCH FOR A waveguide having both an $E$-plane and an $H$-plane distribution, which is highly tapered so as to provide virtually identical radiated $E$- and $H$-plane patterns with low sidelobes, has been underway for over four decades. Excellent technical accounts in chronological order of the pursuit of dual-mode horns (circa 1940 to 1976) in smooth metal-wall waveguide to achieve this end as well as that of later corrugated waveguide investigations (circa 1962 to 1984) have been given by A. W. Love [1], [2] and hence will not be repeated here. Investigations of waveguides with a low-loss dielectric lining of approximately a quarter wavelength thick have likewise been reported [3]–[6], but this approach only works over a narrow bandwidth and is difficult to put into practice since it is difficult to fabricate with the necessary accuracy to prevent excitation of higher order modes. To the authors' knowledge, no analytical investigations of absorber-lined guides were performed for this purpose (since, perhaps intuitively, a lossy-wall guide is automatically deemed unattractive as a waveguide) until Andrew Corporation, prompted by their initial "accidental" experimental findings followed by planned experiments, started proprietary analytical investigations in circa 1980–1981 [7], [8].[1] This work then provided the motivation to analyze-construct an absorber-lined conical-feed horn for a horn-reflector antenna [10], [11] for which a patent was filed in 1981 and awarded in 1983 [12]. This antenna provides virtually equal $E$- and $H$-plane patterns across a continuous bandwidth of over 3:1 [11]–[13]. However, it is the analysis of the simpler parallel-plate absorber model that readily provides the "physical insight" into the understanding of why the $E$-plane and $H$-plane tapering phenomenon occurs and it is this analysis, with associated computations, that is concisely reported here.

Manuscript received May 17, 1985, revised February 3, 1986.

The authors are with Andrew Corporation, Orland Park, IL 60462.

IEEE Log Number 8608337.

[1] These early investigations also included that of a metallic parallel-plate guide with a lossy-magnetic lining which can also produce the desired tapering phenomenon (as independently noted recently by C. S. Lee *et al.* [9] for such a lining in a metallic cylinder). However, the physical realization of an absorber lining (lossy-dielectric) is both simpler and more economical than that of a lossy-magnetic lining, and as such, the latter is not discussed here.

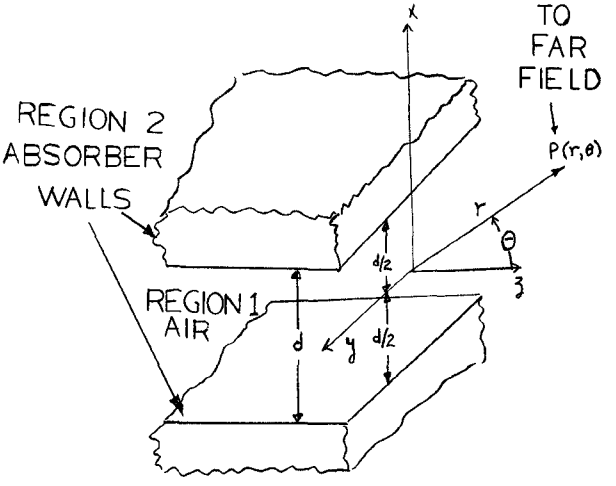


Fig. 1. Geometry of parallel-plate waveguide with absorber walls.

## II. Analysis

Consider then a parallel-plate waveguide having absorber walls spaced a distance $d$ apart and air filled between the walls, as depicted in Fig. 1. The absorber walls are characterized by the complex dielectric constant $\epsilon_r^v = \epsilon_r^1 (1 - j \tan\delta)$, where $\epsilon_r^1$ is the real part of the dielectric constant and $\tan\delta$ is the loss tangent. It is well known that the wave equations to be solved for the TM and TE cases are as shown in Table I, where there the subscript 1 denotes region 1 ($|x| \leqslant (d/2)$, $|z| \leqslant \infty$) and the subscript 2 region 2 ($|x| \geqslant (d/2)$, $|z| \leqslant \infty$), with $k$ being the wave number in region 1 (free space): $k = \omega\sqrt{\mu_v \epsilon_v} = 2\pi/\lambda_v$, $\lambda_v$ being the wavelength in unbounded free space (and $\mu_v$, $\epsilon_v$, and $\eta_v = \sqrt{\mu_v/\epsilon_v}$ are the permeability, permittivity, and characteristic impedance, respectively, of free space) and where $\exp[j\omega t - \gamma_z]$ variation is understood (where $\gamma = \alpha + j\beta$ is the complex propagation factor in the $z$ direction, with the subscripts $m$ for the TM mode and $e$ for the TE mode utilized). The solutions to these wave equations are straightforward to obtain and are also shown in Table I, where here we seek only those solutions having transverse fields which are symmetrical (i.e., even, denoted by superscript $e$) with respect to $x$ (since only a symmetrical transverse source will be used for excitation). The char-

0018-9480/86/0700-0761$01.00 ©1986 IEEE

TABLE I

FIELD EXPRESSIONS AND CHARACTERISTIC (EIGEN-VALUE) EQUATIONS FOR SYMMETRICAL $TM^e$ AND $TE^e$ MODES IN PARALLEL-PLATE WAVEGUIDE WITH ABSORBER WALLS

| QUANTITY | $TM^e$ MODES | $TE^e$ MODES |
|---|---|---|
| WAVE EQUATION, REGION 1 | $\nabla^2 E_{z1} + k^2 E_{z1} = 0$ | $\nabla^2 H_{z1} + k^2 H_{z1} = 0$ |
| WAVE EQUATION, REGION 2 | $\nabla^2 E_{z2} + k^2 \epsilon_r^v E_{z2} = 0$ | $\nabla^2 H_{z2} + k^2 \epsilon_r^v H_{z2} = 0$ |
| AXIAL FIELDS, REGION 1 | $E_{z1} = E_o \cdot \sin(\beta_{xm} x)$ | $H_{z1} = H_o \cdot \sin(\beta_{xe} x)$ |
| AXIAL FIELDS, REGION 2 | $E_{z2} = \frac{x}{\lvert x\rvert} E_o \sin(h_m) \cdot \exp\left[-\alpha_{xm}(\lvert x\rvert - \frac{d}{2})\right]$ | $H_{z2} = \frac{x}{\lvert x\rvert} H_o \sin(h_e) \cdot \exp\left[-\alpha_{xe}(\lvert x\rvert - \frac{d}{2})\right]$ |
| TRANSVERSE FIELDS, REGION 1 | $E_{x1} = Z_{TM1} \cdot H_{y1} = -E_o \cdot (\frac{\gamma_m}{\beta_{xm}}) \cdot \cos(\beta_{xm} x)$ | $E_{y1} = -Z_{TE} \cdot H_{x1} = jH_o \cdot (\frac{k}{\beta_{xe}}) \eta_v \cdot \cos(\beta_{xe} x)$ |
| TRANSVERSE FIELDS, REGION 2 | $E_{x2} = Z_{TM2} \cdot H_{y2} = -E_o (\frac{\gamma_m}{\alpha_{xm}}) \sin(h_m) \cdot \exp\left[-\alpha_{xm}(\lvert x\rvert - \frac{d}{2})\right]$ | $E_{y2} = Z_{TE} \cdot H_{x2} = jH_o (\frac{k}{\alpha_{xe}}) \eta_v \sin(h_e) \cdot \exp\left[-\alpha_{xe}(\lvert x\rvert - \frac{d}{2})\right]$ |
| WAVE NO. RELATION, REGION 1 | $\gamma_m^2 = \beta_{xm}^2 - k^2$, $(\gamma_m \equiv \alpha_m + j\beta_m)$ | $\gamma_e^2 = \beta_{xe}^2 - k^2$, $(\gamma_e \equiv \alpha_e + j\beta_e)$ |
| WAVE NO. RELATION, REGION 2 | $\alpha_{xm}^2 = -(\gamma_m^2 + k^2 \epsilon_r^v)$ | $\alpha_{xe}^2 = -(\gamma_e^2 + k^2 \epsilon_r^v)$ |
| CHAR. WAVE IMP., REGION 1 | $Z_{TM1} = (-j\gamma_m)/(\omega \epsilon_v)$ | $Z_{TE} = (j\omega\mu_v)/\gamma_e$ |
| CHAR. WAVE IMP., REGION 2 | $Z_{TM2} = (-j\gamma_m)/(\omega \epsilon_v \epsilon_r^v)$ | $Z_{TE} = (j\omega\mu_v)/\gamma_e$ |
| CHAR. (EIGEN-VALUE) EQUATION | $h_m^2[(\epsilon_r^v)^2 \tan^2(h_m) + 1] = -(k\frac{d}{2})^2(\epsilon_r^v - 1)$ | $h_e^2[\tan^2(h_e) + 1] = -(k\frac{d}{2})^2(\epsilon_r^v - 1)$ |
| | NOTE: $h_m \equiv \beta_{xm}\frac{d}{2} = h_{mR} + jh_{mI}$ | NOTE: $h_e \equiv \beta_{xe}\frac{d}{2} = h_{eR} + jh_{eI}$ |
| GUIDE WAVELENGTH | $\lambda_{gm} = (\pi d)/\left\{\left[B_m + (B_m^2 + 4h_{mR}^2 h_{mI}^2)^{1/2}\right]/2\right\}^{1/2} \equiv \frac{2\pi}{\beta_m}$ | $\lambda_{ge} = (\pi d)/\left\{\left[B_e + (B_e^2 + 4h_{eR}^2 h_{eI}^2)^{1/2}\right]/2\right\}^{1/2} \equiv \frac{2\pi}{\beta_e}$ |
| | NOTE: $B_m \equiv -h_{mR}^2 + h_{mI}^2 + (k\frac{d}{2})^2$ | NOTE: $B_e \equiv -h_{eR}^2 + h_{eI}^2 + (k\frac{d}{2})^2$ |
| GUIDE ATTENUATION (DB/$\lambda_v$) | $DBW_m = [8.686(2\lambda_{gm}\lambda_v) h_{mR} h_{mI}]/(\pi d^2)$ | $DBW_e = [8.686(2\lambda_{ge}\lambda_v) h_{eR} \cdot h_{eI}]/(\pi d^2)$ |
| | NOTE: $DBW_m \equiv 8.686 \cdot (\alpha_m \lambda_v)$ | NOTE: $DBW_e \equiv 8.686 \cdot (\alpha_e \lambda_v)$ |
| WAVE NO. - REGION 2 | $\alpha_{xm} = [\epsilon_r^v \cdot h_m \cdot \tan(h_m)]/(\frac{d}{2})$ | $\alpha_{xe} = [h_e \cdot \tan(h_e)]/(\frac{d}{2})$ |
| ABSORBER ATTENUATION (DB/$\lambda_v$) | $DBA_m \equiv 8.686 \cdot \lambda_v \cdot$ REAL-PART $(\alpha_{xm})$ | $DBA_e \equiv 8.686 \cdot \lambda_v \cdot$ REAL-PART $(\alpha_{xe})$ |
| SURFACE WAVE IMPEDANCE | $Z_{STM} \equiv \mp(E_{z1}/H_{y1})\lvert_{x=\pm d/2} = -j\eta_v \cdot h_m \tan(h_m)/(k\frac{d}{2})$ | $Z_{STE} \equiv \pm(E_{y1}/H_{z1})\lvert_{x=\pm\frac{d}{2}} = j\eta_v (k\frac{d}{2})/[h_e \tan(h_e)]$ |
| RADIATION FIELDS (x-z PLANE) | $E_\theta = \gamma_v H_\phi \sim \int_{-d/2}^{+d/2} E_{x1}(x) \cdot \exp[jkx \sin(\theta)]\, dx$ | $E_\phi = -\gamma_v H_\theta \sim \int_{-d/2}^{+d/2} E_{y1}(x) \cdot \exp[jkx \sin(\theta)]\, dx$ |

acteristic (i.e., eigenvalue) equations governing the eigenvalues ($h_m = h_{mR} + jh_{mI}$ for $TM^e$ modes and $h_e = h_{eR} + jh_{eI}$ for $TE^e$ modes) are then as given[2] in Table I.

Using the expressions in Table I, we can then compute the guide wavelength $\lambda_g$, the axial attentuation DBW (in engineering units, decibels per free-space wavelength for ease of interpretation), and the attenuation in the $x$-direction in the absorber wall, DBA (also in engineering units) for both the TM and TE modes (for which the above quantities have the subscripts $m$ and $e$, respectively), once we solve the characteristic-equations for $h_m$ and $h_e$. Note that a knowledge of DBA is important since it will reveal the effect of using a finite absorber lining (backed by metal walls) in place of an infinite absorber wall, as is discussed below.

## III. Special Case of Perfectly Conducting Walls

Prior to reporting the computed results we note that, as a test case, if $\tan\delta$ is allowed to increase beyond limit (representing the case of perfectly conducting walls) then $|\epsilon_r^v|$ approaches infinity and the expressions of Table I reduce to those of a TEM mode (i.e., $h_m = \beta_{xm} = 0$, $\gamma_m = jk$, $\lambda_{gm} = \lambda_v$, $Z_{TM1} = \eta_v$, $E_{x1} = \eta_v \cdot H_{y1} \sim e^{-jkz}$, $E_{z1} = E_{z2} = E_{x2} = H_{y2} = 0$) for the TM case and to those of the $TE_{10}$ mode (i.e., $h_e = \pi/2$, $\gamma_e = jk$, $\lambda_{ge} = \lambda_v$, $Z_{TE1} = \eta_v$, $E_{y1} = -\eta_v \cdot H_{x1} \sim e^{-jkz}$, $H_{z1} = H_{z2} = E_{y2} = H_{x2} = 0$) for the TE case, as should be.

[2] Note that these equations, though not explicitly derived in the work of Marcuse [14], can be obtained from it. For example, if, in that work, we let $n_1 = 1$ and $n_2 = n_3 = n = \sqrt{\epsilon_r^v}$ and use (1.3–66) p. 16 and then (1.2–14) p. 6 to eliminate $\gamma$ and square both sides, we obtain the TM characteristic equation of Table I. Similarly, (1.3–39) p. 13 (and, again, (1.2–14) p. 6) of that work gives the TE characteristic equation of Table I. However, Marcuse did not specifically consider the absorber case.

## IV. Desired Value of $\epsilon_r^v$

Now, the purpose of this investigation is to see if the absorber walls can produce highly tapered transverse fields (ideally vanishing at the walls). From Table I we see this is equivalent to asking if a value(s) of $\epsilon_r^v$ can be found such that $h_m$ and $h_e$ either equal $\pi/2$ or approach it, since then a pure cosine distribution (with an infinite edge taper) will result. This is the basic goal (we note that $h_m = h_e = \pi/2$ corresponds to a cutoff wavelength of $\lambda_c = 2\pi/\beta_x = 2d$).

Analytical examination of the TM and TE characteristic equations of Table I discloses that a sufficient condition to achieve this is to make: (a) $\epsilon_r^1 > 1$, (b) $0 < \tan\delta < 1$, and (c) $kd \gg 1$ (see Appendix I). The physical interpretation of (a) and (b) is to have the waveguide walls made of lossy dielectric (where neither the values of $\epsilon_r^1$ or $\tan\delta$ are critical) which is the case for typical absorber materials (foam impregnated with carbon) which have representative values of $1.1 \lesssim \epsilon_r^1 \lesssim 2.2$ and $0.05 \lesssim \tan\delta \lesssim 0.7$ with a value of $\epsilon_r^1 = 1.4$ and $\tan\delta = 0.4$ being one which can be readily made. The physical significance of (c) is that the wall spacing be many free-space wavelengths.

TABLE II
ROOTS OF $h_m$ AND $h_e$ FOR SYMMETRICAL $TM^e_{10}$ AND $TE^e_{10}$ DOMINANT MODES IN PARALLEL-PLATE WAVEGUIDE WITH ABSORBER WALLS

| | | | | $TM^e_{10}$ ROOTS | | | | | | $TE^e_{10}$ ROOTS | | | | | |
|---|---|---|---|---|---|---|---|---|---|---|---|---|---|---|---|
| Case | $\epsilon_r'$ | $\tan\delta$ | $d$ | $f_{GHz}$ | $h_{mR}$ | $h_{mI}$ | $\lambda_{gm}$ | $\lambda_v$ | DBW | DBA | $h_{eR}$ | $h_{eI}$ | $\lambda_{ge}$ | $\lambda_v$ | DBW | DBA |
| ABS4 | 1.40 | 0.40 | 85.5" | 3.95 | 1.5672 | 0.0315 | 2.9906 | 2.9901 | 0.00832 | 20.712 | 1.5610 | 0.01651 | 2.9906 | 2.9901 | 0.00019 | 20.712 |
| ABS6 | 1.40 | 0.40 | 85.5" | 6.175 | 1.5682 | 0.0202 | 1.9128 | 1.9127 | 0.000888 | 20.715 | 1.5646 | 0.0119 | 1.9128 | 1.9127 | 0.000052 | 20.715 |
| ABS11 | 1.40 | 0.40 | 85.5" | 11.20 | 1.5697 | 0.01114 | 1.0546 | 1.0545 | 0.000215 | 20.716 | 1.5674 | 0.00656 | 1.0546 | 1.0545 | 0.000009 | 20.716 |
| ABS41 | 1.40 | 0.01 | 85.5" | 3.95 | 1.5696 | 0.0287 | 2.9906 | 2.9901 | 0.00691 | 0.6031 | 1.5659 | 0.0276 | 2.9906 | 2.9901 | 0.00029 | 0.603 |
| ABS61 | 1.40 | 0.01 | 85.5" | 6.175 | 1.5702 | 0.0247 | 1.9128 | 1.9127 | 0.000620 | 0.6036 | 1.5703 | 0.0127 | 1.9128 | 1.9127 | 0.000077 | 0.6037 |
| ABS111 | 1.40 | 0.01 | 85.5" | 11.20 | 1.5708 | 0.01364 | 1.0546 | 1.0545 | 0.000018 | 0.6040 | 1.5706 | 0.0097 | 1.0546 | 1.0545 | 0.000013 | 0.6011 |
| ABS48 | 1.40 | 0.40 | 20.0" | 3.95 | 1.5681 | 0.1327 | 2.9982 | 2.9901 | 0.02543 | 20.809 | 1.5270 | 0.0759 | 2.9898 | 2.9901 | 0.01436 | 20.822 |
| ABS86 | 1.40 | 0.40 | 20.0" | 6.175 | 1.5580 | 0.0835 | 1.9149 | 1.9127 | 0.006616 | 20.676 | 1.5433 | 0.04952 | 1.9148 | 1.9127 | 0.00367 | 20.679 |
| ABS113 | 1.40 | 0.40 | 20.0" | 11.20 | 1.5649 | 0.0574 | 1.0549 | 1.0545 | 0.001314 | 20.705 | 1.5550 | 0.02773 | 1.0549 | 1.0545 | 0.00066 | 20.705 |
| ABS42 | 1.40 | 0.40 | 10.0" | 3.95 | 1.5013 | 0.2586 | 3.0208 | 2.9901 | 0.1938 | 20.217 | 1.4793 | 0.1435 | 3.0303 | 2.9901 | 0.1059 | 20.313 |
| ABS62 | 1.40 | 0.40 | 10.0" | 6.175 | 1.5363 | 0.1686 | 1.9704 | 1.9127 | 0.05264 | 20.531 | 1.5130 | 0.09560 | 1.9209 | 1.9127 | 0.02900 | 20.559 |
| ABS112 | 1.40 | 0.40 | 10.0" | 11.20 | 1.5501 | 0.0960 | 1.0560 | 1.0545 | 0.00902 | 20.568 | 1.5404 | 0.0544 | 1.0560 | 1.0545 | 0.0052 | 20.571 |

## V. COMPUTATIONS OF EIGENVALUES AND TRANSVERSE FIELDS

Fortran programs have been written to solve the characteristic TM and TE equations for the eigenvalues $h_m$ and $h_e$. Specific cases of interest ran were for: $\epsilon_r^1 = 1.40$, $\tan\delta = 0.4$ with $d = 85.5$ in, 20.0 in, and 10.0 in for $f = 3.95$, 6.175, and 11.2 GHz since these values are of extreme commercial interest (as they approximate those used with a conical waveguide having a maximum diameter of 85.5 in and a minimum diameter of 10 in which comprises part of the conical-horn feed for the previously mentioned horn-reflector antenna, as discussed in more detail in Section IX below).

The results for these cases are tabulated in Table II and indeed show that the dominant mode roots of $h_m$ and $h_e$ are both near $\pi/2$ (the more so at the highest frequency and largest wall spacing, since this is the case having the largest value of $(kd)$). For the sake of interest, (to help answer the question of the effect of finite absorber thickness), the case of $\tan\delta = 0.01$ (for $d = 85.5$ in, with all other parameters held the same) was also run (which also gives $h_m$ and $h_e$ roots near $\pi/2$) as tabulated in Table II. Not shown are other cases (for the same $d$ and frequency range as above) having wide ranges of $\epsilon_r^1$ ($\epsilon_r^1 > 1$) and $\tan\delta$ ($0 < \tan\delta < 1$) which also give roots of $h_m$ and $h_e$ near $\pi/2$, and show the insensitivity of the solution ot $\epsilon_r^1$ and $\tan\delta$.

The transverse-field distributions ($E$-plane, $TM_{10}$ case, $20\log_{10}|E_{x1}(0)/E_{x1}(x)|$dB, and $H$-plane, $TE_{10}$ case, $20\log_{10}|E_{y1}(0)/E_{y1}(x)|$dB), for the cases of Table II are concisely shown in Fig. 2 and readily show that the ideal cosine distribution is approached for the highest frequency and largest wall spacing cases (i.e., $kd$ increasing); the best case (ABS11) being for 11.2 GHz and 85.5 in, Fig. 2(c), for which both the $E$-plane and $H$-plane edge-tapers exceed 40 dB. The worst case (Case ABS42) is that for the lowest frequency and smallest wall spacing, i.e., 3.95 GHz and 10 in, Fig. 2(g), where only 11-dB $E$-plane and 15-dB $H$-plane edge tapers result, respectively.

## VI. RADIATION PATTERN COMPUTATIONS

The expressions for the radiation patterns in the $xz$-plane are also given in Table I for both the $E$-plane (TM case) and $H$-plane (TE) cases and consist of the integration of

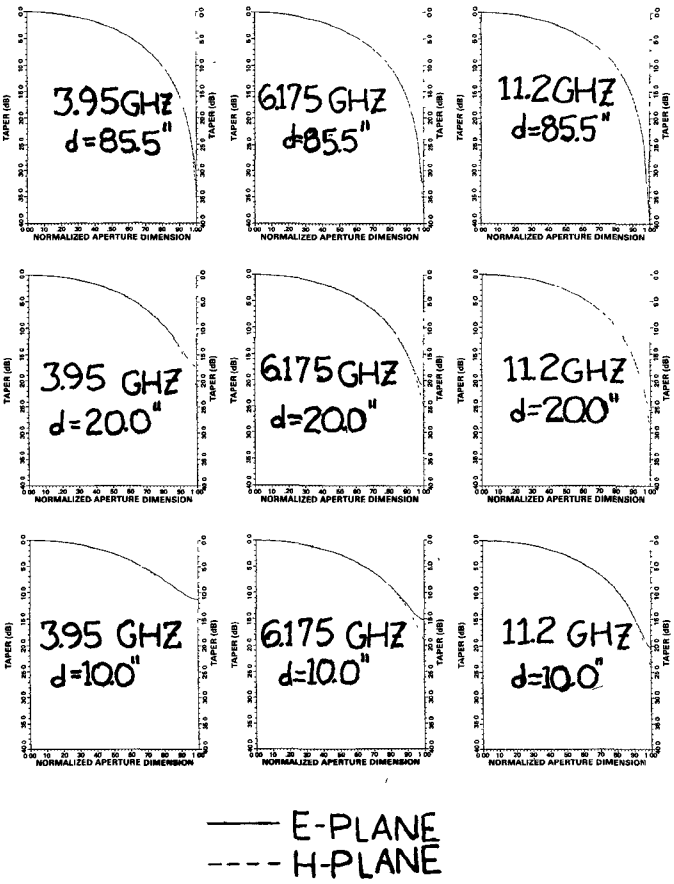


Fig. 2. $E$- and $H$-plane aperture distributions of parallel-plate waveguide with absorber walls ($\epsilon_r^1 = 1.40$, $\tan\delta = 0.40$). Note: Abscissa = normalized aperture dimension = $[|x|/(d/2)]$.

the $E_{x1}$ or $E_{y1}$ fields, respectively, over the aperture of the guide, where the radiation from the absorber face is neglected (as is justified for the highly tapered fields in region 1 for $d = 85.5$ in). Performing this integration numerically for the $TM^e_{10}$ and $TE^e_{10}$ modes gives the results of Fig. 3(a)–(c) for the $d = 85.5$ in cases at 3.95, 6.175, and 11.2 GHz, respectively. The corresponding metallic-plate guide patterns ($\sin U/U$ for the $E$-plane (TM) case, solid curves, and $\cos U/[1-(2U/\pi)^2]$, dotted curves, for the $H$-plane (TE) cases, where $U = (\pi d \sin\theta)/(2\lambda_v)$ are shown in Fig. 4(a)–(c). It is seen that the $E$-plane patterns for the absorber case (Fig. 3) have much lower sidelobes than is the case for the corresponding metal wall case (Fig. 4) and that they are virtually equal to the $H$-plane patterns, with each being close to the metal-wall $H$-plane patterns of Fig. 4.

## VII. EFFECT OF FINITE ABSORBER THICKNESS

We note from Table II that for either the relatively high-loss cases ($\tan\delta = 0.4$) or the relatively low-loss cases ($\tan\delta = 0.01$) that the guide wavelength $\lambda_g$ is only slightly larger than $\lambda_v$ (indicating a fast wave) and that DBW, the attenuation down the guide, i.e., in the $z$ direction, is extremely small (especially at the highest frequency and largest wall spacing). This is because the region 1 fields at the walls are so highly tapered. We also note that the

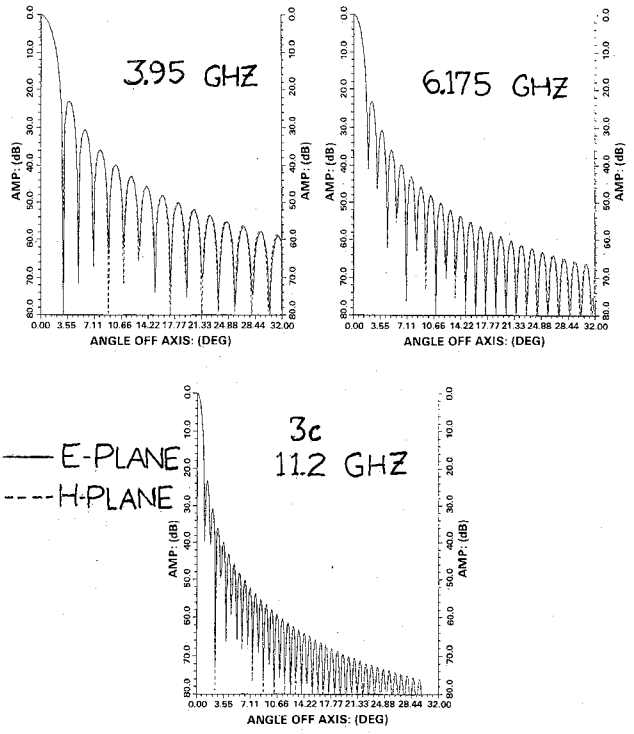


Fig. 3. $E$- and $H$-plane radiation patterns of parallel-plate waveguide with absorber walls ($\epsilon_r^1 = 1.40$, $\tan\delta = 0.4$, $d = 85.5$ in).

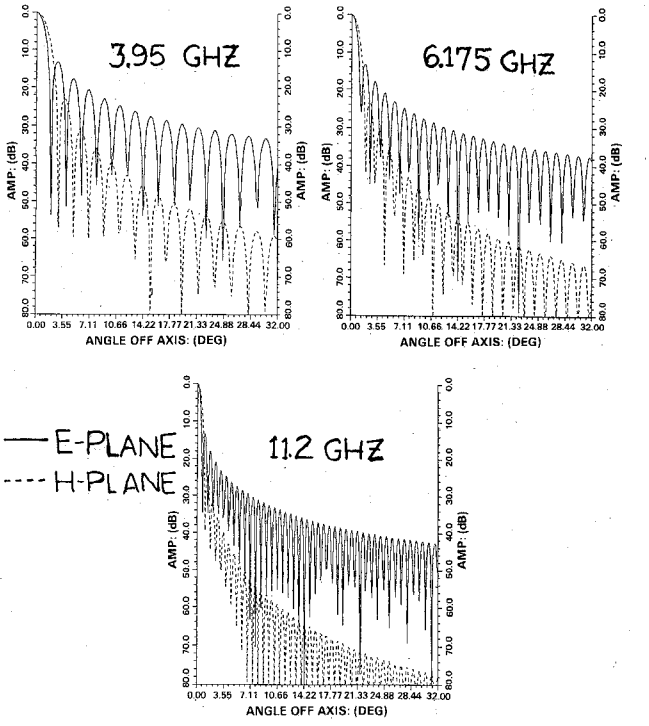


Fig. 4. $E$- and $H$-plane radiation patterns of parallel-plate waveguide with metal walls ($d = 85.5$ in).

attenuation DBA in the absorber, i.e., in the $x$ direction is very large for the $\tan\delta = 0.40$ case (e.g., about 7, 10, and 20 dB/in for 3.95, 6.175, and 11.2 GHz, i.e., cases ABS4, ABS6, and ABS11, respectively), but is small for the $\tan\delta = 0.01$ case (e.g., about 0.2, 0.3, and 0.6 dB/in at 3.95, 6.175, and 11.2 GHz, i.e., cases ABS41, ABS61, and ABS111, respectively).

We now can answer the question: What will be the effect of using a finite absorber wall-thickness $T$ (backed, say, by a metal wall)? Intuitively, if the thickness $T$ and the attenuation DBA is such as to give a roundtrip attenuation of, say, 10 to 20 dB or more, then one would expect that the performance would differ negligibly from that for $T$ being infinite. Choosing this 10- to 20-dB range, then for $\tan\delta = 0.4$, it gives a required $T$ range for this case of: 0.71 in $\lesssim T \lesssim$ 1.42 in (at 3.95 GHz, the worse case, since at higher frequencies, a given $T$ will then give more than 10 to 20 dB). Of course, for the lower loss tangent cases, $T$ would have to be correspondingly larger (e.g., for the $\tan\delta = 0.01$ case 24 in $\lesssim T \lesssim$ 49 in, i.e., impractically large). Thus a reasonably high $\tan\delta$ is necessary to keep $T$ to practical values (e.g., $\tan\delta = 0.40$ gives $T$ about 1 in). In other words, one would then expect that for frequencies of 3.95 GHz or greater if a parallel plate waveguide made of metal walls of spacing of about 10 in or more is lined with an absorber of about 0.71 to 1.4 in thickness or more and has $\epsilon_r^1 = 1.4$ and $\tan\delta = 0.4$, it should behave about the same as one with infinite walls made of the same absorber and having the same wall spacing. That this is indeed so is shown exactly by analyzing such a structure [8]. Furthermore, the same is true for a metallic conical-horn lined with such an absorber [10]–[12]. In essence, it was redundant to analyze either of these latter structures once the infinite absorber-wall case was done, in so far as demonstrating the field-tapering principle involved; however, these models do enable one to more accurately determine, for given values of $\epsilon_r^1$, $\tan\delta$, $d$, and frequency the minimum value of $T$ that should be used.

## VIII. Physical Explanation of Operation

The fact that the absorber walls (or absorber lining on a metal backing, if the roundtrip attenuation in the absorber lining is about 10 to 20 dB or more) can cause a cosine type (highly tapered) distribution for both the $TM_{10}^e$- and $TE_{10}^e$-type modes simultaneously can be physically attributed to the ability of the absorber surface (wall)-impedance to act like a corrugated ("$\lambda/4$") surface. Thus, the surface impedance of the $TM_{10}$ mode $Z_{STM}$ approaches an infinite capacitive reactance while, simultaneously, that of the $TE_{10}$ mode $Z_{STE}$ approaches zero (like a perfect conductor), as seen by examining these expressions in Table I for the case of $h_m$ and $h_e$ being slightly less than $\pi/2$ (as is the case, via Table II). It is also noted that $Z_{STM}\, Z_{STE} = \eta_v^2$, thus, as $Z_{STM}$ approaches infinity, $Z_{STE}$ must approach zero.

## IX. Actual Application

As briefly mentioned above, if the spacing between the absorber walls $d$ is allowed to gradually taper from a maximum spacing (say 85.5 in) down to a very small spacing (say several inches), then it approximates that of an actual conical-horn feed. The actual conical feed extends down to a circular/waveguide (excited by the domi-

nant $TE_{11}$ mode, which constitutes the transverse-symmetrical exciting source) of several inches in diameter and has a smooth metal wall from that diameter up to a diameter of 10 in or greater where it is absorber-lined from there up to the 85.5 in diameter. Analysis [10]–[12] of the actual metallic cone with absorber lining is much more involved than that of the simpler parallel-plate model reported here, but also shows that the transverse field distribution is highly tapered (it approaches the $J_0$ [2.405 $x/(d/2)$] type $HE_{11}$ mode distribution, where $J_0(Y)$ = Bessel function of order zero and argument $Y$, which resembles a cosine function vanishing at the absorber walls, $x = \pm d/2$). A feed horn of this type is being used to excite a horn-reflector paraboloid antenna of about a 10-ft projected diameter which produces virtually equal $E$- and $H$-plane radiation patterns about equal to those of the $H$-plane pattern of a metallic smooth wall-horn reflector of the same diameter. Furthermore, it does this over the continuous frequency range of at least 3.7 to 11.7 GHz [13]. Thus, the physical transverse-field tapering-phenomenon, as predicted by the simpler parallel-plate model, does indeed occur.

It should also be mentioned that the measured transverse field distribution in the above feed horn at its maximum diameter (85.5 in) was relatively "clean" indicating that no surface (i.e., slow waves) or, also, that any higher order mode fast waves were present to any significant extent. Both of these mode types may be excited at the starting diameter junction of the smooth wall-absorber wall interface. Indeed, the absorber wall acts to highly attenuate any slow waves since these waves have their maximum value at the surface of the absorber wall. The fact that they were unobserved obviated the necessity of obtaining their corresponding characteristic equation and finding its roots; similarly the roots of the higher order mode fast waves were not required.

## X. Conclusions

The analysis and computation of the symmetrical-dominant $TM_{10}^e$ and $TE_{10}^e$ modes, which can propagate through and radiate from a parallel-plate waveguide having absorber-walls, have been given. These findings show that for a wall spacing large compared to a free-space wavelength, the surface impedance of these absorber walls simultaneously approach an infinite capacitive reactance for the $TM_{10}^e$ case and zero for the $TE_{10}^e$ case just like "quarter wave" corrugated walls with the added feature that this holds for virtually an unlimited bandwidth. This surface impedance leads to highly tapered (cosine-type) transverse field distributions, accompanied by low axial attenuation at a phase velocity slightly greater than the speed of light and produces virtually equal $E$-plane ($TM_{10}$) and $H$-plane ($TE_{10}$) radiated patterns having low side lobes similar to that of the $H$-plane ($TE_{10}$) pattern of a smooth metallic wall of the same wall spacing. Having established the physical basis of operation, the parallel-plate model studied was then used to explain the operation of an actual metallic-conical absorber-lined horn-reflector antenna.

## Appendix I
## Sufficient Conditions on $\epsilon_r^v$ and $kd$ to Obtain $h_m$ and $h_e$ near $\pi/2$

### A. $TM^e$ Case

We first note

$$\tan h_m = [\sin(2h_{mR}) + j\sinh(2h_{mI})] / [\cos(2h_{mR}) + \cosh(2h_{mI})] \quad \text{(AI-1)}$$

and then let $h_{mR}$ be close to $\pi/2$ and $h_{mI}$ close to zero, so $\sin(2h_{mR}) \doteq 0$, $\cos(2h_{mR}) \doteq -1$, $\sinh(2h_{mI}) \doteq 2h_{mI}$ and $\cosh(2h_{mI}) \doteq 1 + 2\cdot h_{mI}^2$. This gives $\tan h_m = +j/h_{mI}$, which, since $h_{mI}$ is very small, is a very large imaginary number. Thus, the characteristic equation for the $TM_{10}$ mode (via Table I) becomes

$$[(\pi/2) + jh_{mI}]^2\left\{\left[-(\epsilon_r^v)^2/h_{mI}^2\right] + 1\right\} = -(kd/2)^2(\epsilon_r^v - 1). \quad \text{(AI-2)}$$

Since $\epsilon_r^v = \epsilon_r^1(1 - j\tan\delta)$, (AI−2) gives two equations (by equating the real parts to each other and the imaginary parts to each other) which become (retaining only the most significant terms of order $h_{mI}^{-2}$)

$$(\pi/2)^2(\epsilon_r^1)^2(1 - \tan^2\delta)/h_{mI}^2 \doteq (kd/2)^2(\epsilon_r^1 - 1) \quad \text{(AI-3a)}$$

$$2(\pi/2)^2\epsilon_r^1/h_{mI}^2 \doteq (kd/2)^2 \quad \text{(AI-3b)}$$

respectively, where $h_{mI}$ approaches zero. Now if $\epsilon_r^1 > 1$ and $0 < \tan\delta < 1$ then both sides of (AI-3a) are positive and this fact together with that of both sides of (AI-3b) being positive (since $\epsilon_r^1$ is positive) means both (AI-3a) and (AI-3b) can be satisfied simultaneously, especially for $(kd)$ very large (since then, $h_{mI}$ will become closer to zero). Thus, the conditions of: $\epsilon_r^1 > 1$, $0 < \tan\delta < 1$ and $kd \gg 1$ are sufficient to cause $h_m$ to approach $\pi/2$ (this is also seen, computationally, from the results of Table II where $h_{mR}$ is slightly less than $\pi/2$ and $h_{mI}$ is small, each approaching their limiting values of $\pi/2$ and zero, respectively, as $kd$ increases).

### B. $TE^e$ Case

In a similar way, the characteristic equation for the $TE_{10}^e$ modes of Table I can be examined analytically to show that the same conditions as above are sufficient to cause $h_{eR}$ to approach $\pi/2$, as is also seen from the computations of Table II.

## References


[1] A. W. Love, *Electromagnetic Horn Antennas*. New York: IEEE Press, 1976.

[2] A. W. Love, "Horn antennas," in *Antenna Engineering Handbook*, R. C. Johnson and H. Jasik, Eds., 2nd edition. New York: McGraw-Hill, 1984.

[3] J. W. Carlin and P. D'Agostino, "Low-loss modes in dielectric-lined waveguide," *Bell System Tech. J.*, vol. 50, no. 5, pp. 1631–1639, May–June 1971.

[4] J. W. Carlin, "A relation for the loss characteristics of circular electric and magnetic modes in dielectric-lined waveguide," *ibid*, vol. 50, no. 5, pp. 1639–1644, May–June 1971.

[5] P. J. B Clarricoats, A. M. B. Al-Hariri, A. D. Olver, and K. B. Chan, "Low attenuation characteristics of dielectric-lined wave-

guide," *Electron. Letters*, vol. 8, no. 16, pp. 407–409, Aug. 1972.
[6] C. Dragone, "Attenuation and radiation characteristics of the $HE_{11}$-mode," *IEEE Trans. Microwave Theory Tech.*, vol. MTT-28, no. 7, pp. 704–710, July 1980.
[7] C. M. Knop and D. W. Matz, "Propagation through and radiation from a parallel-plate waveguide having absorber walls," Andrew Corp. Eng. Rep., RP-967, June 1980.
[8] C. M. Knop and D. W. Matz, "Propagation through and radiation from a parallel-plate waveguide having absorber walls or metal walls with a dielectric lining," Andrew Corporation Eng. Rep., RP-974, Mar. 1981.
[9] C. S. Lee, S. L. Chuang, and S. W. Lee, "A simple version of corrugated waveguide: Smooth-walled circular waveguide coated with lossy magnetic material," in *Proc. 1985 IEEE/AP-S Symp.*, Vancouver, BC
[10] C. M. Knop and Y. B. Cheng, "The fields produced by a horn having an arbitrary half-angle and arbitrary wall impedance," Andrew Corp. Eng. Rep., RP-974, Dec. 19, 1980.
[11] C. M. Knop, Y. B. Cheng, and E. L. Ostertag, "On the fields in a conical-horn having an arbitrary wall impedance," to be published.
[12] U.S. Patent, 4,410,892, Oct. 18, 1983.
[13] Andrew Corp. Antennas SHX10A and SHX10B, Bulletin 1281E.
[14] D. Marcuse, *Theory of Dielectric Optical Waveguides*. New York: Academic Press, 1974, ch. 1.

✠

**Charles M. Knop** (SM'66) was born in Chicago, IL. He received the B.S.E.E., M.S.E.E., and Ph.D.E.E. degrees from the Illinois Institute of Technology, the latter in 1963.

Initially he solicited/performed U.S. Government R/D in the technical areas of: X- and Ka-band waveguide slotted-arrays; surface wave antennas; waveguide-component development; H.F. propagation; artificial dielectrics; dielectric coated-slotted-cylinder antennas; dielectric-rod antennas; helical antennas; radar cross section and transient-electromagnetic propagation, at both midwest (IITRI, Bendix, Hallicrafters) and west coast (Hughes, NESCO) companies. In the late-60's, Dr. Knop made the intentional transition to commercial-telecommunication-antenna research/development by joining Andrew Corporation, where he is presently Chief Scientist/Director—Antenna Research. Here he, with his associates, have developed (using G.O., P.O., G.T.D., and advanced programming techniques) state of the art microwave-reflector antennas and associated corrugated horns. These antennas include: symmetrical prime-fed paraboloids, conical-horn reflectors, conventional Cassegrains, symmetrical shaped dual-reflectors and/or offset Gregorians/Cassegrains, offset prime-fed parabolas, etc., for use as both terrestrial microwave radio-relay antennas and as satellite-ESA's (Earth Station Antennas). Virtually all these antenna types are currently in production (the symmetrical shaped Gregorian ESA's for C- and Ku-bands meet the stringent 2° satellite-spacing requirements and provide 85- to 90-percent efficiency). Associated studies of microwave propagation phenomenon (fading, group delay, etc.) as well as development of HF, VHF, and UHF antennas of various types are also ongoing.

In the early-70's Dr. Knop taught all the graduate-electromagnetic/antenna courses at IIT. He has been a reviewer of papers for the IEEE-AP, IEEE-MTT and Radio Science since about 1963 and has authored over 48 technical papers in these same and related journals as well as chapter 30 on Microwave-Relay Antennas in the Antenna Engineering Handbook (McGraw-Hill, 1984, second-edition of Johnson–Jasik). He also holds over six patents in the antenna field.

He is a member of URSI-Commission B, Eta Kappa Nu, Sigma Xi, Tau Beta Pi, Rho Epsilon, and the New York Academy of Sciences and is listed in International Who's Who in Engineering and Who's Who in Technology Today.

✠

**Yuk-Bun Derek Cheng** (S'72—M'77) was born in Shantou City, Guangdong Province, China, in 1950. He received the B.S.E.E. degree from West Virginia Institute of Technology, Montgomery, WV, in 1974 and the M.S.E.E. degree from West Virginia University, Morgantown, WV, in 1976.

From 1974 to 1977, he was a Graduate Research Assistant at the Department of Electrical Engineering of West Virginia University, where he concentrated on the application of GTD to the analysis of aircraft antenna radiation for Microwave Landing System. In 1977, he joined Andrew Corporation, where he has since been engaged in research and development activities on Earth Station and Terrestrial Microwave Antennas. Currently he is a Section Leader—Antenna Analysis.

Mr. Cheng was the receipient of the Radio Technical Commission for Aeronautics 1976 William E. Jackson Award. He is a member of Xigma Xi, Eta Kappa Nu, Tau Beta Pi, Phi Kappa Phi, and the Association for Computing Machinery. He is listed in Personalities of America, Who's Who in the Midwest, and Who's Who in the World. Presently, he is serving as Chairman of the IEEE Chicago Joint Chapter of AP/MTT Societies.

✠

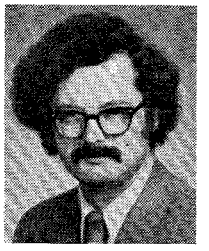

**Edward L. Ostertag** (M'71) was born in Springfield, IL, in 1948. He received the B.S.E.E. and M.S.E.E. degrees from the University of Illinois, Champaign-Urbana in 1969 and 1971, respectively.

In the summer of 1970, he held an Andrew Fellowship Award and upon receipt of his M.S.E.E. joined Andrew Corporation as a Design-Engineer rising to Antenna Design-Manager in 1979, a position he still maintains. He has made significant contributions to antenna design-prototype development in shaped-reflectors, corrugated horns, four-port combiners, etc. He is responsible for the maintenance-updating of Andrew's VAX-11/780 computer, both software, graphics, and hardware.